

Estimation of Coolant Void Reactivity for CANDU-NG Lattice using DRAGON and Validation using MCNP5 and TRIPOLI-4.3

Ramamoorthy Karthikeyan, Romain Le Tellier and Alain Hébert
*École Polytechnique de Montréal, 2900 Boulevard Édouard-Montpetit, Montréal,
Québec, H3T 1J4, Canada*

Abstract

The Coolant Void Reactivity (CVR) is an important safety parameter that needs to be estimated at the design stage of a nuclear reactor. It helps to have an a priori knowledge of the behavior of the system during a transient initiated by the loss of coolant. In the present paper, we have attempted to estimate the CVR for a CANDU New Generation (CANDU-NG) lattice, as proposed at an early stage of the Advanced CANDU Reactor (ACR) development. We have attempted to estimate the CVR with development version of the code DRAGON, using the method of characteristics. DRAGON has several advanced self-shielding models incorporated in it, each of them compatible with the method of characteristics. This study will bring to focus the performance of these self-shielding models, especially when there is voiding of such a tight lattice. We have also performed assembly calculations in 2 x 2 pattern for the CANDU-NG fuel, with special emphasis on checkerboard voiding. The results obtained have been validated against Monte Carlo codes MCNP5 and TRIPOLI-4.3.

KEYWORDS: *Coolant void reactivity, CANDU-NG lattice, DRAGON, MCNP5, TRIPOLI-4.3, Checkerboard voiding, Resonance self-shielding*

1. Introduction

The CANDU New Generation (CANDU-NG) lattice was proposed at an early stage of the Advanced CANDU Reactor (ACR) development[©] and is now used for academic benchmarking [1]. It does not comprise the detailed engineering features of the ACR[©] that guarantee a negative CVR under all conditions. The CANDU-NG fuel bundle is a 43 element CANFLEX[©] design which is one of the several proposals considered for the futuristic reactor to be built by Canada. The CANDU-NG lattice has some salient design features like central dysprosium pin, light water as coolant, square lattice pitch of 22 cm and a large calandria tube diameter, in order to reduce the heavy water moderator inventory. There was also a requirement that the design caters to higher burnup in comparison to the present CANDU6 fuel, and hence there was a consideration for enriched uranium fuel. Several studies have been performed earlier to estimate the CVR for the evolving ACR[©] design [2].

Corresponding author, Tel. 514-3404711 ext 4120, Fax. 514-340-4192,
E-mail: karthikeyan.ramamoorthy@polymtl.ca

© - AECL

The central pin of the 43 rod cluster has dysprosium (4.6 %) in natural uranium. The central pin and seven pins in ring 1 are thicker (inner/outer diameter-0.627/0.675 cm) compared to fourteen pins in ring 2 and twenty-one pins in ring 3 (inner/outer diameter-0.533/0.575 cm). The fuel density of the inner eight pins is higher (10.12 g/cc) in comparison to the outer 35 pins (9.825 g/cc). The pressure tube dimension is the same as that of CANDU-6. An important geometrical change for ACR[®] type lattice is the increase in the calandria tube inner/outer diameter (7.5/7.8 cm) in comparison to CANDU-6 (6.45/6.59 cm). As a result the air gap is much larger and the moderator volume is further reduced. The coolant is light water and the moderator is heavy water, and we have considered the air gap to be filled with helium gas. Fig. 1 gives the cross section of a 43 element fuel assembly and a single pin with 4 layers (50%, 30%, 15% and 5% volume) considered in each fuel pin, which is based on the recommendations by Santamarina [3]. The subdivision is made in order to effectively predict the distributed self-shielding effects within a fuel pin. The mesh-splitting of Fig. 1 produces 389 regions and 60 outer surfaces, each of them corresponding to an unknown of the main flux calculation. No mesh-splitting of the moderator is required for the self-shielding calculation, leading to 44 regions and 4 outer surfaces in this case.

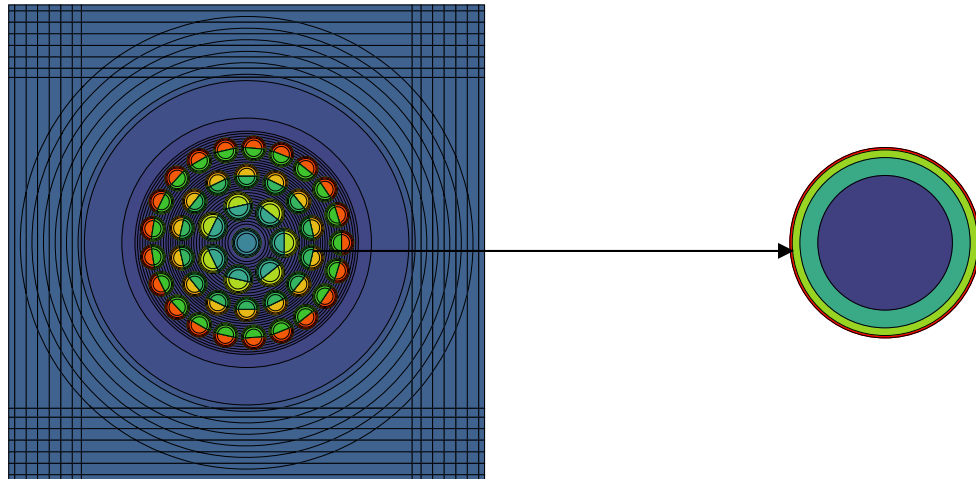


Fig. 1: Cross section of CANDU-NG unit cell and single pin

2. Brief description of code and nuclear data

A total of 27 nuclides from JEF-2.2 evaluation were considered for the analysis. NJOY99.90 [4] together with the DRAGR [5] module has been used for the generation of a multigroup cross section library in DRAGLIB format for analysis using DRAGON. The weighting spectrum that was chosen to collapse the cross sections to 172 groups correspond to analytic thermal + 1/E + fission. A Compact ENDF (ACE) libraries needed for analyses using MCNP5 [6] have also been generated using the NJOY99.90 code. The PENDF tapes that are produced during the library generation process have been used for analysis using TRIPOLI-4.3 [7]. The lattice calculations were performed using a development version of the DRAGON code [8] for the above mentioned reference cell. In the present paper, we will be focusing mainly on the performance of advanced self-shielding models based on equivalence in dilution principle or a subgroup approach on estimation of CVR for tight pitch lattices and in the presence of strong burnable absorbers like dysprosium. Under equivalence in dilution models, we used the

Generalised Stamm'ler model [9] with or without Riemann integration and Nordheim model [10]. Among the subgroup approaches, we have used the Ribon extended and the statistical self-shielding models, which are both compatible with a characteristics solution of the subgroup equations [11].

Two sets of studies have been carried out as part of the present work. In the first set, CVR will be estimated for a single CANDU-NG unit cell using DRAGON. This study will include two varieties, where we will be considering, natural uranium/dysprosium in natural uranium, in the central pin. It will help in understanding the effect of dysprosium during coolant voiding, and performance of self-shielding models in the presence of strong burnable absorbers. The outer boundary of the unit cell has been considered as square and isotropic boundary condition has been applied on it. The fuel pins were split into two in an inward/outward fashion. This splitting was done not only in terms of regions for the flux calculations but also in terms of correlated resonant mixtures for the space-dependent self-shielding treatment. This refinement of the self-shielding treatment has a noticeable effect (~ 40 pcm) on the k_{∞} when the cell is voided. It also improved the resonant capture in the outer ring of fuel and has an overall effect of about 25 pcm on the CVR. This splitting in terms of regions for the flux calculation has also a noticeable effect on the thermal fission rate.

As the coolant is light water, a fine mesh was found mandatory. Each of the 3 annular regions corresponding to the different ring of fuel pincells is divided in 12 annular submeshes. A coarser mesh was used for the heavy water moderator. It consists in annuli close to the calandria tube and cartesian meshes near the boundary. These meshes were used to correctly represent the flux gradients caused by heterogeneous neighboring cells. The corners of the square cell have been discretized, as depicted in Fig. 1. The method of characteristics [12] was used for the multigroup flux integration.

Finally we considered the estimation of CVR for an assembly in 2×2 pattern, which includes complete voiding and checkerboard voiding. Isotropic translation boundary condition has been applied on the external surfaces of the lattice. Note that there is no approximation on the internal surfaces that couple the cells. Consequently, the effect of the approximated boundary conditions can be deciphered by comparing the single cell calculations to the 2×2 assembly calculations. Tracking of assembly in 2×2 pattern is made possible by use of the NXT: tracking module, which has been developed at École Polytechnique [13]. The cross section of a 2×2 CANDU-NG assembly is shown in Fig. 2.

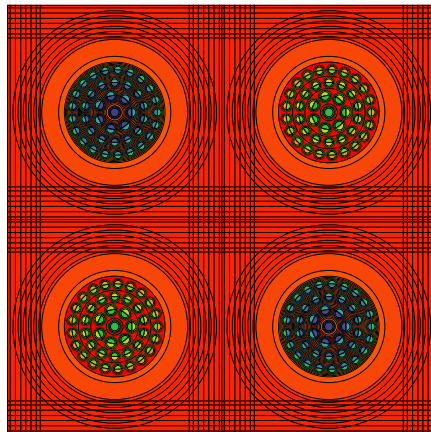


Fig. 2: Cross section of 2x2 CANDU-NG assembly

In the present work there is a special emphasis on checkerboard voiding calculation, which has been performed by considering void in the diagonal cells and coolant in the other two cells. In an earlier study [2] it has been mentioned that the CVR estimated for a checkerboard lattice for ACR[®] is higher than that obtained for complete voiding. In a previous study, checkerboard voiding estimation has been carried out using Version 3 of DRAGON [14] for a CANDU-6 lattice, but with modifications to the basic lattice, where square pins were considered instead of annular pins [15].

In the present study the results obtained using DRAGON has been validated against that obtained using Monte Carlo codes MCNP5 and TRIPOLI-4.3. A total of 10 million neutron histories were tracked using MCNP5 and TRIPOLI-4.3. This validation process will help in identifying the appropriate self-shielding model that can be recommended for analysis of tight pitch lattices using DRAGON. Apart from comparing the CVR values, we have also compared the capture rate in the resolved resonance energy group '677.29 eV to 2.7679 eV'

3 Results and Discussions

As a first step, the CANDU-NG cell was analyzed using Monte Carlo codes MCNP5 and TRIPOLI-4.3. The reference values obtained using these codes are presented in Table 1. Four sets of calculations were performed. The sets included two varieties of fuel and two coolant states. The two varieties of fuel include natural uranium/ dysprosium in natural uranium in the central pin at two coolant densities of 0.714 g/cc and 0.001 g/cc each. The k_{∞} was estimated for each of the states and the CVR for each variety was estimated using the Equation 1:

$$CVR = \frac{1}{k_{\infty}(S_1)} - \frac{1}{k_{\infty}(S_2)} \quad (1)$$

where S_1 and S_2 corresponds to presence(0.714 g/cc) and absence(0.001 g/cc) of coolant respectively. The deviation for CVR was obtained using Equation 2.

$$Deviation = \sqrt{\frac{\delta_1^2}{k_{\infty}(S_1)^4} + \frac{\delta_2^2}{k_{\infty}(S_2)^4}} \quad (2)$$

where δ_1 is the standard deviation for $k_{\infty}(S_1)$ obtained using MCNP5, while δ_2 is the standard deviation for $k_{\infty}(S_2)$. As mentioned earlier, this study is being performed to qualitatively and quantitatively assess the performance of advanced self-shielding models for the CVR calculation on a tight pitched lattice in the presence of strong burnable absorbers.

In the following discussions, we will be using the following notations to represent the various self-shielding models. The generalized Stamm'ler model (GSM) without Livolant-Jeanpierre normalization (LJN) [9] will henceforth be referred to as 'GSM0-NOLJ' and that with LJN will be referred to as 'GSM0-LJ'. The generalized Stamm'ler model with Nordheim model (GSM1) and no LJN will henceforth be referred to as 'GSM1-NOLJ' and that with LJN will be referred to as 'GSM1-LJ'. The generalized Stamm'ler model with Nordheim model and Riemann Integration (GSM2) and no LJN will henceforth be referred to as 'GSM2-NOLJ' and that with LJN will be referred to as 'GSM2-LJ'. The statistical self-shielding model and the Ribon extended self-shielding model will be henceforth referred to as 'SUBG' and 'RIB' respectively. The estimation of CVR for the first variety with central pin having natural uranium will henceforth be referred to as 'V1' and that with dysprosium in natural uranium in central pin will be referred to as 'V2'.

Table 1 gives the k_{∞} values and CVR obtained using MCNP5, TRIPOLI-4.3 and DRAGON, for a single CANDU-NG lattice for 'V1' and 'V2', with and without coolant. It can be observed in Table 1 that the results obtained using MCNP5 and TRIPOLI-4.3 match well. It can however be noted that with identical number of neutron histories, the standard deviation on the k_{∞} obtained using TRIPOLI-4.3 is higher than that of MCNP5. Hence, we have used the results obtained using MCNP5 to validate the results obtained using DRAGON.

It can be seen from Table 1 that the results obtained using the self-shielding models in DRAGON systematically under-predict basic k_{∞} values with respect to that obtained using MCNP5. The results obtained using 'GSM1-NOLJ' show the maximum deviation, for both 'V1' and 'V2' for both cooled and voided states. k_{∞} values predicted by GSM0 are better than GSM1 and GSM2 when NOLJ option is considered. This trend is reversed when LJ option is considered. However, the under prediction by all the GSM models is reduced when LJ option is considered. It is interesting to note that GSM2-LJ predicts basic k_{∞} close to that of MCNP5 in the presence of coolant. Another interesting trend when there is voiding is that the GSM models without LJJ predict k_{∞} close to that of MCNP5 when compared to GSM models with LJJ. When LJJ is used, the trend is reversed for GSM2 for 'V1' and for all the GSM models for 'V2'. However, the subgroup models have a uniform trend of increased under-prediction during voiding for both 'V1' and 'V2'. The CVR is estimated to be positive for 'V1' and 'V2', but the magnitude is lower in case of 'V2'. It can be seen from Fig. 3 that the capture rate is almost doubled when one considers dysprosium in the central pin. The capture rate gets further enhanced during voiding and thus Dy plays a crucial role in lowering the CVR. The CVR predicted using the various self-shielding models incorporated in DRAGON, are in close agreement with that estimated using MCNP5.

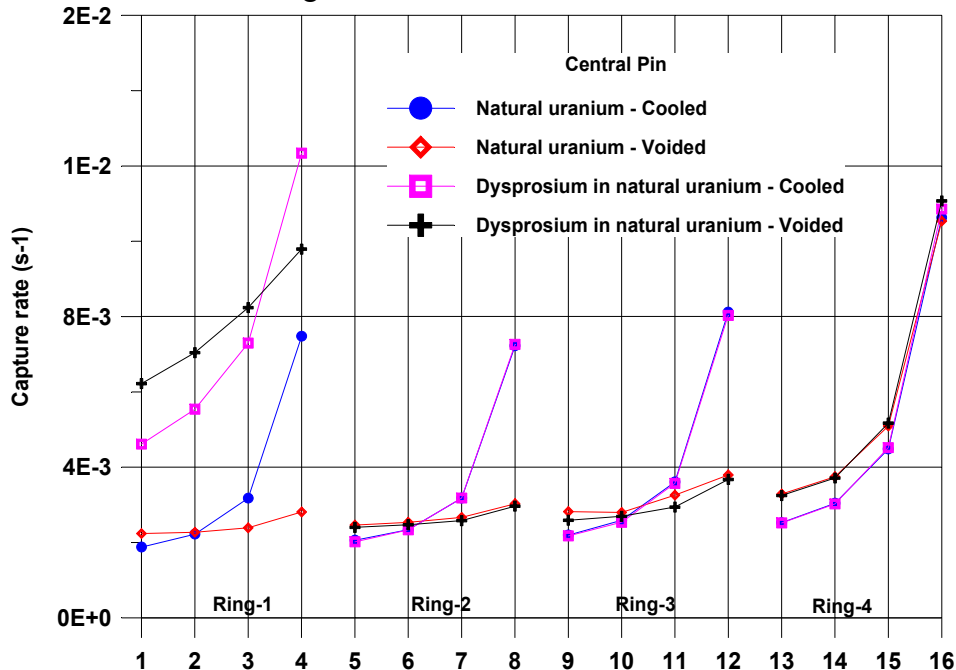


Fig. 3 – Capture rate in four layers of pins in four rings

Table 2 compares the capture rate for 'V2', in resolved resonance energy group obtained using MCNP5 and all the self-shielding models in DRAGON. It can be seen that the models

based on a subgroup approach predicts the capture rate better than the models based on equivalence in dilution. Even though the k_{∞} predicted by GSM2LJ is better during voiding, it can be noted that the capture rate is over predicted. It was noted that the subgroup approach ('SUBG') based on physical probability tables seems to predict the basic k_{∞} , CVR and reaction rates better than all other models. This trend has been observed before on simpler validation tests [11]. The Stamm'ler method is based on very crude approximations related to the calculation of the equivalent dilution in each resonant region and each resonant energy group. The subgroup method with physical probability tables is now considered as the recommended tool in state-of-the-art lattice codes and is compatible with the characteristics method. Finally, the Ribon extended method is more expensive and is required only in situations where the mutual shielding phenomenon is important. We have thus used 'SUBG' model for assembly calculations in 2x2 pattern.

Table 3 gives the k_{∞} values for assembly calculation in 2x2 pattern, obtained using MCNP5, TRIPOLI-4.3 and DRAGON for fully cooled, fully voided and checkerboard voiding states. Translation boundary condition is applied on all the parallel surfaces in order to truly reflect the physical phenomena when there is a possibility of checkerboard voiding. It can be seen that the k_{∞} and CVR values for 2x2 pattern matches quite well with that obtained for a single cell in Table 1. When all the four cells are cooled, it can be noticed that the difference from single cell calculation, using DRAGON, is about 15pcm while it is about 40pcm when all cells are voided. It is interesting to note that these differences are about half those obtained when one compares calculations with isotropic and specular boundary conditions for cooled and voided states using MCNP5 (about 30pcm and 80pcm). This is totally coherent as each cell in a 2x2 assembly has two outer surfaces out of four for which the isotropic/uniform boundary conditions are applied. One can expect that with an exact treatment of the boundary condition (i.e. a specular tracking obtained using translation boundary condition), DRAGON results will be closer to MCNP5 in estimation of CVR. This capability is currently under development in NXT: [13].

It is interesting to note from Table 3 that the CVR value during checkerboard voiding for 'V1' is lower than that obtained for total coolant voiding. But for 'V2', the CVR obtained for checkerboard voiding is higher than that observed when there is total voiding. It can be seen from Table 3 that this trend is also observed using the code DRAGON. Table 4 compares the capture rate in resolved resonance energy group obtained using MCNP5 and DRAGON for the three states – all 4 cells cooled, voided and checkerboard voiding. It can be observed that the capture rate estimated using 'SUBG' model in DRAGON is predicted within a few percents of values obtained using MCNP5. The maximum discrepancy of 15% is found in the outermost layer of pins in second ring.

Conclusions

Coolant void reactivity has been estimated for CANDU-NG lattice using various self-shielding models incorporated in a development version of the DRAGON code. The obtained results have been validated using Monte Carlo codes MCNP5 and TRIPOLI-4.3. It was observed that the self-shielding model based on subgroup approach using physical probability tables predicts the basic k_{∞} , CVR and reaction rates better than all the other models. This model was used for performing the assembly calculation in 2x2 pattern and the CVR for checkerboard

voiding state was estimated. This calculation using DRAGON was made possible by the introduction of a new tracking module NXT: developed at École Polytechnique de Montréal. Using DRAGON, we have obtained the trend of a higher CVR for checkerboard voiding state when compared to complete voiding state for CANDU-NG lattice with dysprosium in the central pin.

Acknowledgements

This work was supported by a grant from the Natural Science and Engineering Research Council of Canada. The authors are grateful to Guy Marleau for providing us with an alpha version of NXT: at an early stage of development and for helping us in setting the geometries.

References

1. P. S. W. Chan, K. T. Tsang and D. B. Buss, "Reactor Physics of NG CANDU", paper presented at 22nd Annual Conference of the Canadian Nuclear Society, Toronto, Ontario, Canada, June 10-13, 2001.
2. C. A. Cotton, D. Lee et. al, "Physics Analysis of Coolant Voiding in the ACR-700 Lattice", paper presented at 2005 ANS Annual Meeting - The Next 50 years : Creating opportunities, San Diego, California, June 5-9, 2005.
3. A. Santamarina, C. Collignon and C. Garat, "French Calculation Schemes for Light Water Reactor Analysis", paper presented at PHYSOR 2004 -The Physics of Fuel Cycles and Advanced Nuclear Systems: Global Developments, Chicago, Illinois, April 25-29, 2004.
4. R. E. Macfarlane and D. W. Muir, "NJOY99.0 Code System for Producing Pointwise and Multigroup Neutron and Photon Cross Sections from ENDF/B Data", Los Alamos National Laboratory, New Mexico, U.S.A, PSR-480/NJOY99.0, March 2000.
5. A. Hébert and H. Saygin, "Development of DRAGR for the Formatting of DRAGON Cross-section Libraries, paper presented at the Seminar on NJOY-91 and THEMIS for the Processing of Evaluated Nuclear Data Files", NEA Data Bank, Saclay, France, April 7-8 (1992).
6. X-5 Monte Carlo Team, "MCNP- A General Monte Carlo N-Particle Transport Code, Version 5", Report LA-CP-03-0245, April 24, 2003.
7. J. P Both and Y. Penelieu, "The Monte Carlo code TRIPOLI-4 and its first benchmark interpretations", Proc. on Int. Conf. on the Physics of Reactors. PHYSOR 96, Mito, 1996.
8. G. Marleau, A. Hébert and R. Roy, "A User Guide for DRAGON", Institut de génie nucléaire, École Polytechnique de Montréal, Montréal, Québec, Report IGE-174 Rev.6, Dec. 19, 2003.
9. A. Hébert and G. Marleau, "Generalization of the Stamm'ler Method for the self-shielding of resonant isotopes in arbitrary geometries", Nucl. Sci. Eng., **108**, p. 230-239, 1991.
10. A. Hébert, "Revisiting the Stamm'ler self-shielding model", paper presented at 25th CNS Annual Conference, Toronto, Canada, June 6-9, 2004.
11. A. Hébert, "A Presentation of the Ribon Extended Self-shielding Model", Nucl. Sci. Eng., **151**, No. 1, p. 1-24, September 2005.

12. R. Le Tellier, A. Hébert, and G. Marleau, “The implementation of a 3 D characteristics solver for the generation of incremental cross sections for reactivity devices in a CANDU reactor”, paper submitted to Topical Meeting on Advances in Nuclear Analysis and Simulation, Vancouver, Canada, September 10-14, 2006.
13. G. Marleau, “New Geometries Processing in DRAGON: The NXT: Module”, Report IGE-260, École Polytechnique de Montréal, Montréal, 2005.
14. G. Marleau, A. Hébert and R. Roy, “A User Guide for DRAGON Version DRAGON000331 Release 3.04”, Institut de génie nucléaire, École Polytechnique de Montréal, Montréal, Québec, Report IGE-174 Rev.5, (2000); see also A. Hébert, G. Marleau and R. Roy, “Application of the lattice code DRAGON to CANDU analysis”, *Trans. Am. Nucl. Soc.*, **72**, 335 (1996); see also G. Marleau, A. Hébert and R. Roy, *New Computational Methods Used in the Lattice Code DRAGON*, Topical Meeting on Advances in Reactor Physics, Charleston, SC, March 1992.
15. F. Talebi and G. Marleau, “Evaluation the coolant void reactivity of assemblies of CANDU-6 lattices”, paper presented at 26th Annual Conference of the Canadian Nuclear Society, Toronto, Ontario, Canada, June 12-15, 2005.

Table 1: Comparison of k_{∞} for single CANDU-NG lattice

Model	Central pin (Natural Uranium)			Central pin – (Dysprosium in Natural Uranium)		
	k_{∞} (Cooled)	k_{∞} (Voided)	CVR (mk)	k_{∞} (Cooled)	k_{∞} (Voided)	CVR (mk)
MCNP5	1.30449±0.00016	1.32867±0.00017	13.95±0.13	1.25556±0.00017	1.26374±0.00018	5.16±0.16
TRIPOLI-4.3	1.30368±0.00039	1.32788±0.00038	13.98±0.31	1.25538±0.00037	1.26330±0.00038	4.99±0.33
GSM0NOLJ	1.295636(8.85) ⁺	1.321776(6.89)	15.26(-1.31) [#]	1.247138(8.42)	1.257248(6.49)	6.45(-1.29)
GSM1NOLJ	1.293526(10.96)	1.319230(9.44)	15.06(-1.11)	1.245127(10.43)	1.254910(8.83)	6.26(-1.11)
GSM2NOLJ	1.294951(9.54)	1.319816(8.85)	14.55(-0.60)	1.246381(9.18)	1.255327(8.41)	5.72(-0.56)
GSM0LJ	1.298398(6.09)	1.323106(5.56)	14.38(-0.43)	1.249887(5.67)	1.258674(5.07)	5.59(-0.43)
GSM1LJ	1.299090(5.40)	1.322908(5.76)	13.86(0.09)	1.250488(5.07)	1.258555(5.18)	5.13(0.03)
GSM2LJ	1.303145(1.34)	1.324415(4.26)	12.32(1.63)	1.254105(1.46)	1.259785(3.95)	3.60(1.56)
SUBG	1.301370(3.12)	1.324880(3.79)	13.64(0.32)	1.252515(3.05)	1.260125(3.61)	4.82(0.33)
RIB	1.301625(2.86)	1.324436(4.23)	13.23(0.72)	1.252757(2.80)	1.259701(4.04)	4.40(0.76)

⁺ ΔK (in mk) = (k_{∞} (MCNP5) - k_{∞} (model))

[#] ΔCVR (in mk) = (CVR(MCNP5) - CVR(model))

Table 2: Comparison of the capture rate in the resolved resonance energy group for single CANDU-NG lattice

Ring	Layer	Central Pin – Natural Uranium									Central pin – (Dysprosium in Natural Uranium)								
		Capture rate(s ⁻¹)	A	B	C	D	E	F	G	H	Capture rate(s ⁻¹)	A	B	C	D	E	F	G	H
1	1	4.6127E-03±0.037	18.66	9.74	11.17	18.30	6.59	9.25	5.18	5.40	6.2208E-03±0.030	9.35	4.39	6.34	9.19	2.49	5.93	3.61	3.79
	2	5.5395E-03±0.037	10.14	6.20	6.96	8.88	2.79	5.42	3.05	2.99	7.0400E-03±0.030	3.90	1.21	2.75	3.16	-0.32	3.94	1.26	1.37
	3	7.2948E-03±0.046	-8.67	-2.48	-0.55	-10.41	-2.11	2.51	1.37	1.04	8.2389E-03±0.036	-5.69	-4.26	-2.56	-6.87	-3.25	0.44	-0.76	-0.73
	4	1.2344E-02±0.070	-42.72	-4.54	-4.59	-44.13	-1.93	-1.23	0.00	0.02	9.7927E-03±0.049	-17.36	4.50	0.60	-18.72	7.17	3.76	0.05	0.22
2	5	2.0176E-03±0.054	29.71	12.48	11.06	28.95	7.98	4.90	1.91	2.34	2.4022E-03±0.045	15.27	5.74	5.27	15.14	5.23	4.23	1.66	2.24
	6	2.3350E-03±0.057	19.97	9.81	7.98	18.73	5.59	2.32	1.22	1.15	2.4713E-03±0.047	14.28	5.94	5.42	14.12	2.60	1.58	2.23	2.74
	7	3.1801E-03±0.075	-6.93	-1.33	-1.42	-8.25	0.20	-0.87	0.58	0.04	2.5813E-03±0.055	10.99	5.85	5.75	10.81	10.01	10.86	4.52	4.94
	8	7.2628E-03±0.111	-57.80	-25.06	-21.07	-58.51	-22.89	-17.16	-2.62	-2.57	2.9633E-03±0.095	-2.50	1.91	3.75	-2.68	5.09	8.45	15.36	15.62
3	9	2.1742E-03±0.061	30.89	14.44	12.81	29.85	9.53	6.10	2.15	2.50	2.5898E-03±0.050	17.45	8.02	7.43	17.19	6.82	7.16	1.63	2.17
	10	2.5368E-03±0.063	19.01	11.09	9.18	17.60	7.66	3.80	1.25	1.10	2.6958E-03±0.052	15.11	7.64	7.07	14.80	3.62	2.72	1.89	2.33
	11	3.5682E-03±0.084	-11.34	-1.18	-0.51	-12.69	1.50	1.91	0.09	-0.58	2.9404E-03±0.070	7.08	4.79	5.12	6.75	9.88	8.82	2.45	2.74
	12	8.0317E-03±0.121	-59.38	-21.80	-17.67	-60.09	-19.67	-13.73	-3.49	-3.25	3.6744E-03±0.117	-13.46	-4.60	-1.86	-13.74	-1.88	2.58	9.35	9.83
4	13	2.5182E-03±0.059	30.74	16.06	13.96	29.16	9.64	5.06	1.29	1.47	3.2472E-03±0.049	15.88	10.59	9.09	15.16	7.23	4.62	0.54	0.84
	14	3.0229E-03±0.061	16.06	12.71	10.06	14.13	8.37	3.12	0.94	0.41	3.7094E-03±0.052	5.13	8.19	6.55	4.37	5.24	1.43	0.40	0.19
	15	4.5187E-03±0.082	-18.47	-0.11	0.32	-20.13	2.01	1.87	0.44	-0.65	5.1698E-03±0.071	-22.55	-1.78	-0.65	-23.18	-0.44	1.85	-2.06	-2.77
	16	1.0857E-02±0.109	-65.01	-16.92	-13.87	-65.80	-15.37	-11.01	-0.83	-0.70	1.1074E-02±0.100	-63.27	-27.79	-24.16	-63.58	-26.58	-22.39	-5.27	-5.07

Deviation in % using {A-GSM0NOLJ; B-GSM1NOLJ; C-GSM2NOLJ; D-GSM0LJ; E-GSM1LJ; F-GSM2LJ; G-SUBG; H-RIB}

Table 3: Comparison of k_{∞} for assembly in 2x2 pattern for CANDU-NG

Central pin	Code	k_{∞} (A)*	k_{∞} (B)#	CVR(A-B)	k_{∞} (C) ^s	CVR(A-C)
Nat. U	MCNP5	1.30480±0.00016	1.32967±0.00017	14.33±0.13	1.32497±0.00016	11.67±0.13
	TRIPOLI-4.3	1.30368±0.00039	1.32788±0.00038	13.98±0.31	1.32411±0.00038	11.84±0.32
	SUBG	1.301501(3.30)	1.325320(4.35)	13.81(0.53)	1.321484(3.49)	11.62(0.05)
Dysprosium in Natural Uranium	MCNP5	1.25609±0.00017	1.26494±0.00018	5.57±0.16	1.26774±0.00018	7.32±0.16
	TRIPOLI-4.3	1.25530±0.00037	1.26297±0.00039	4.84±0.34	1.26660±0.00037	7.11±0.33
	SUBG	1.252654(3.44)	1.260513(4.43)	4.98(0.59)	1.263947(3.79)	7.13(0.18)

*A – All 4 cells cooled

#B – All 4 cells voided

^sC – Checkerboard voiding

Table 4: Comparison of capture rate in resolved resonance energy group for assembly calculation in 2x2 pattern for CANDU-NG with central pin having Dy in Natural Uranium)

Ring	Layer		Capture rate(s ⁻¹)	A		Capture rate(s ⁻¹)	B		Capture rate(s ⁻¹)	C
1	1	Cooled	2.3100E-03+/-0.053	4.93	Voided	3.0968E-03+/-0.043	3.89	Cooled	2.6629E-03+/-0.048	5.40
	2		2.7796E-03+/-0.053	2.46		3.5029E-03+/-0.043	1.52		3.2168E-03+/-0.049	2.50
	3		3.6598E-03+/-0.065	1.04		4.0835E-03+/-0.051	-0.04		4.2173E-03+/-0.060	1.52
	4		6.3148E-03+/-0.103	-1.87		4.7857E-03+/-0.066	2.67		7.1955E-03+/-0.094	-0.29
2	5		1.0230E-03+/-0.078	0.55		1.2098E-03+/-0.065	0.84		1.1746E-03+/-0.071	1.57
	6		1.1577E-03+/-0.078	2.11		1.2273E-03+/-0.065	2.82		1.3503E-03+/-0.074	1.48
	7		1.5995E-03+/-0.105	0.00		1.2929E-03+/-0.081	4.23		1.8415E-03+/-0.099	0.67
	8		3.6078E-03+/-0.160	-2.21		1.4852E-03+/-0.141	14.60		4.1642E-03+/-0.147	-1.69
3	9		1.1015E-03+/-0.086	0.81		1.2811E-03+/-0.070	2.61		1.2763E-03+/-0.080	1.58
	10		1.2674E-03+/-0.089	1.34		1.3359E-03+/-0.073	2.67		1.5021E-03+/-0.084	-0.19
	11		1.8146E-03+/-0.124	-1.87		1.4337E-03+/-0.093	4.76		2.0892E-03+/-0.112	-0.51
	12		3.9253E-03+/-0.169	-1.18		1.8258E-03+/-0.158	9.86		4.6210E-03+/-0.159	-1.91
4	13		1.2682E-03+/-0.084	0.50		1.6186E-03+/-0.069	0.69		1.4867E-03+/-0.077	1.04
	14		1.5113E-03+/-0.086	0.87		1.8801E-03+/-0.076	-1.15		1.7644E-03+/-0.080	1.82
	15		2.2366E-03+/-0.112	1.44		2.5785E-03+/-0.101	-2.02		2.6624E-03+/-0.106	0.44
	16		5.3172E-03+/-0.153	1.21		5.4176E-03+/-0.141	-3.34		6.4597E-03+/-0.139	-1.74
1	17	Cooled	2.3220E-03+/-0.053	4.39	Voided	3.0908E-03+/-0.043	4.09	Voided	2.5172E-03+/-0.048	4.32
	18		2.7597E-03+/-0.053	3.20		3.4948E-03+/-0.043	1.76		2.8504E-03+/-0.048	1.89
	19		3.6552E-03+/-0.065	1.17		4.0968E-03+/-0.050	-0.36		3.3522E-03+/-0.058	-0.48
	20		6.1635E-03+/-0.099	0.54		4.8308E-03+/-0.066	1.71		3.9895E-03+/-0.076	0.71
2	21		1.0063E-03+/-0.076	2.22		1.2044E-03+/-0.065	1.30		9.7692E-04+/-0.071	1.73
	22		1.1503E-03+/-0.080	2.76		1.2275E-03+/-0.067	2.80		1.0018E-03+/-0.072	2.63
	23		1.5609E-03+/-0.108	2.47		1.3011E-03+/-0.084	3.57		1.0454E-03+/-0.087	5.04
	24		3.5303E-03+/-0.158	-0.06		1.4937E-03+/-0.139	13.95		1.2059E-03+/-0.146	15.06
3	25		1.0989E-03+/-0.086	1.05		1.2937E-03+/-0.071	1.61		1.0575E-03+/-0.081	1.30
	26		1.2788E-03+/-0.091	0.44		1.3385E-03+/-0.073	2.47		1.1032E-03+/-0.086	1.33
	27		1.8265E-03+/-0.121	-2.51		1.4522E-03+/-0.094	3.42		1.1838E-03+/-0.106	3.44
	28		4.0613E-03+/-0.171	-4.49		1.8451E-03+/-0.172	8.71		1.4893E-03+/-0.188	9.88
4	29		1.2548E-03+/-0.082	1.57		1.6069E-03+/-0.070	1.42		1.3371E-03+/-0.079	-0.61
	30		1.5094E-03+/-0.088	1.00		1.8426E-03+/-0.073	0.86		1.5206E-03+/-0.083	-0.30
	31		2.2730E-03+/-0.118	-0.18		2.5824E-03+/-0.102	-2.17		2.0770E-03+/-0.112	-0.71
	32		5.5005E-03+/-0.155	-2.16		5.5332E-03+/-0.144	-5.35		4.4611E-03+/-0.158	-4.03

Deviation in % using {A – All cells cooled; B – All cells voided; C- Checkerboard voiding}